ANL/MSD/CP-99579

# FERROELECTRIC AND PIEZOELECTRIC PROPERTIES OF MOCVD $Pb(Mg_{1/3}Nb_{2/3})O_3$-$PbTiO_3$ EPITAXIAL THIN FILMS*

P. K. Baumann, G. R. Bai, S. K. Streiffer, K. Ghosh, and O. Auciello
Materials Science Division, Argonne National Laboratory, Argonne, IL 60439, USA

S. Stemmer
Dept. of Mech. Engineering and Materials Science, Rice University, Houston, TX 77005, USA

A. Munkholm
Chemistry Division, Argonne National Laboratory, Argonne, IL 60439, USA

Carol Thompson
Department of Physics, Northern Illinois University, DeKalb, IL 60115, and Materials Science Division, Argonne National Laboratory, Argonne, IL 60439, USA

D.-J. Kim, J.-P. Maria, and A. I. Kingon
Dept. of Materials Science and Engineering, North Carolina State University, Raliegh, NC 27695

January 2000



To be submitted for publication to the proceeding of Symposium KK on " Materials Issues for Tunable RF and Microwave Devices" of the MRS 1999 Fall Meeting, Boston, MA, November 29 – December 3, 1999.

*Work supported by the U. S. Department of Energy, BES-Materials Science and Office of Transportation Technologies, under Contract W-31-109-ENG-38.

## DISCLAIMER

## ABSTRACT

We have grown epitaxial $Pb(Mg_{1/3}Nb_{2/3})O_3$ (PMN) and (1-x)($Pb(Mg_{1/3}Nb_{2/3})O_3$)-x($PbTiO_3$) (PMN-PT) thin films by metalorganic chemical vapor deposition at 700 - 780°C on (100) $SrTiO_3$ and $SrRuO_3/SrTiO_3$ substrates. The zero-bias permittivity and loss measured at room temperature and 10 kHz for 220 nm thick pure PMN films were 900 and 1.5%, respectively. For PMN-PT films the small-signal permittivity ranged from 1000 to 1500 depending on deposition conditions and Ti content; correspondingly low values for the zero-bias dielectric loss between 1 and 5% were determined for all specimens. For PMN-PT with x of approximately 0.30-0.35, polarization hysteresis with $P_r \approx 18 \mu C/cm^2$ was obtained. Initial piezoresponse data are discussed.

## INTRODUCTION

Recently there has been significant interest in relaxor-based thin films for dielectric and piezoelectric applications [1]. Lead magnesium niobate and lead magnesium niobate titanate exhibit high dielectric constants and excellent piezoelectric/electrostrictive characteristics [2, 3]. Pure PMN is a relaxor with a temperature maximum of the permittivity that is rather low for practical utility (~ -8°C) [4]; PT is added in solid solution to PMN to obtain a material with a more useful Curie temperature [5], and to set the material near the morphotropic phase boundary for piezoelectric applications. To date several thin film deposition techniques have been employed to produce PMN-PT, including pulsed laser deposition [6-8], sol-gel [9-11], sputter deposition [12], and metal organic chemical vapor deposition (MOCVD) [13]. MOCVD of oxide ferroelectrics has a number of advantages, including good composition control, superior thickness and composition uniformity of the films, high deposition rates, and the possibility to scale the process to large size wafers. To date only very little work has been done on MOCVD grown PMN-PT thin films, and this work has been limited to growth of polycrystalline films with compositions of Ti/(Mg+Nb+Ti) > 25 mol% [13]. In order to optimize the piezoelectric properties of PMN-PT it will be necessary to obtain highly oriented and phase pure material. In this study we report structural and electrical properties of phase pure, epitaxial PMN and PMN-PT thin films deposited on (100) $SrTiO_3$ and $SrRuO_3/SrTiO_3$ substrates by MOCVD.

## EXPERIMANTAL DETAILS

The PMN and PMN-PT thin films were deposited in a horizontal, cold wall MOCVD reactor. Tetraethyl lead, $Pb(C_2H_5)_4$, niobium pentaethoxide, $Nb(OC_2H_5)_5$, solid magnesium β-diketonate, $Mg(C_{11}H_{19}O_2)_2$, and titanium isopropoxide, $Ti(C_3H_7O)_4$, were chosen as the metal ion precursors. Single crystal (001) $SrTiO_3$ substrates were used to optimize the growth and to study the microstructure of the films. For electrical characterization, PMN-PT films were deposited on $(001)_{pseudocubic}$ $SrRuO_3$ films deposited by off-axis sputtering on (001) $SrTiO_3$ substrates [14]. Pt top electrodes were evaporated through a shadow mask onto the samples at 350°C, so as to form capacitor structures. Further details of the deposition process are reported elsewhere [15]. Table I summarizes the general range of deposition conditions over which films with reasonable quality were obtained. Because of the large number of adjustable parameters and, in particular, variations of the solid Mg precursor vapor pressure, different samples were deposited under rather different absolute conditions in order to achieve phase purity. This is reflected in the broad ranges quoted for some parameters.

Table I: Deposition conditions for PMN-PT films

| | | |
|---|---|---|
| Substrate Temperature: | 700-780°C | |
| Reactor Pressure: | 6 Torr | |
| Precursor Temperatures: | Pb: | 28-30C° |
| | Mg: | 120-140°C |
| | Nb: | 78-85°C |
| | Ti: | 30-36°C |
| Pressure in Precursor Chamber: | Pb: | 500-800 Torr |
| | Mg: | 18 Torr |
| | Nb: | 18 Torr |
| | Ti: | 100-200 Torr |
| Carrier Gas Flow Rate ($N_2$): | Pb: | 20-36 SCCM |
| | Mg: | 36-42 SCCM |
| | Nb: | 55-62 SCCM |
| | Ti: | 14-26 SCCM |
| Oxygen Flow Rate: | 400 SCCM | |
| Background Gas Flow Rate ($N_2$):: | 200 SCCM | |
| Deposition Rate: | 4-6nm/min. | |

Film Ti content x was estimated based on the relative precursor parameters and deposition rates for the PMN and PT end members. Ti content was also estimated by measurement of film refractive index, which has been demonstrated to be a simple linear function of the refractive indices of the end members for other perovskite solid solutions [16]. X-ray diffraction (XRD) and transmission electron microscopy were used for structural characterization of the PMN and PMN-PT thin films; TEM results will be discussed elsewhere [17]. Room temperature electrical characterization to determine permittivity and loss tangent as a function of electric field were performed at 10 kHz and 0.1Vrms oscillation level using an HP4192A impedance analyzer. Hysteresis loops were measures on a Radiant RT6000 test system. A Digital Instruments DI3000 scanning probe microscope (SPM) was employed to analyze the surface morphology and roughness of the films. Double beam laser interferometry was used to determine piezoelectric coefficients [18].

## RESULTS AND DISCUSSION

It was found that XRD $\theta$-$2\theta$ scans of optimized PMN-PT/$SrTiO_3$ films exhibited only (001) peaks of the $SrTiO_3$ substrate and the pseudocubic PMN-PT, as shown in Figure 1 a) and b) for films with thicknesses of approximately 300nm. Samples deposited on $SrRuO_3$/$SrTiO_3$ were found to behave identically. However, for non-optimized (lead poor) conditions an impurity peak was found at $2\theta \sim 43.3°$, corresponding to a d-spacing of ~0.2 nm. Also, some samples exhibited x-ray signatures generally attributed to lead oxide. Investigation of these impurity phases is reported in [17]. Synchrotron x-ray

scattering at the Advanced Photon Source and cross-sectional TEM demonstrated that the orientation relationship between film and substrate was purely cube-on-cube, that is $(001)_{film}\|(001)_{substrate}$ and $(100)_{film}\|(100)_{substrate}$. X-ray scattering on a 200nm pure PMN film on $SrTiO_3$ yielded an out-of-plane rocking curve $\Delta\theta$ of the PMN (001) reflection of approximately 0.1°, while the in-plane mosaic spread $\Delta\phi$ of the PMN (111) was approximately 0.8°. The lattice parameters determined from these same reflections were $d_{(001)}$=0.4063nm and $d_{(100)}$=0.4037nm. This indicates that some tetragonality is imposed on the films, most likely from the temperature dependent misfit with the underlying substrate.

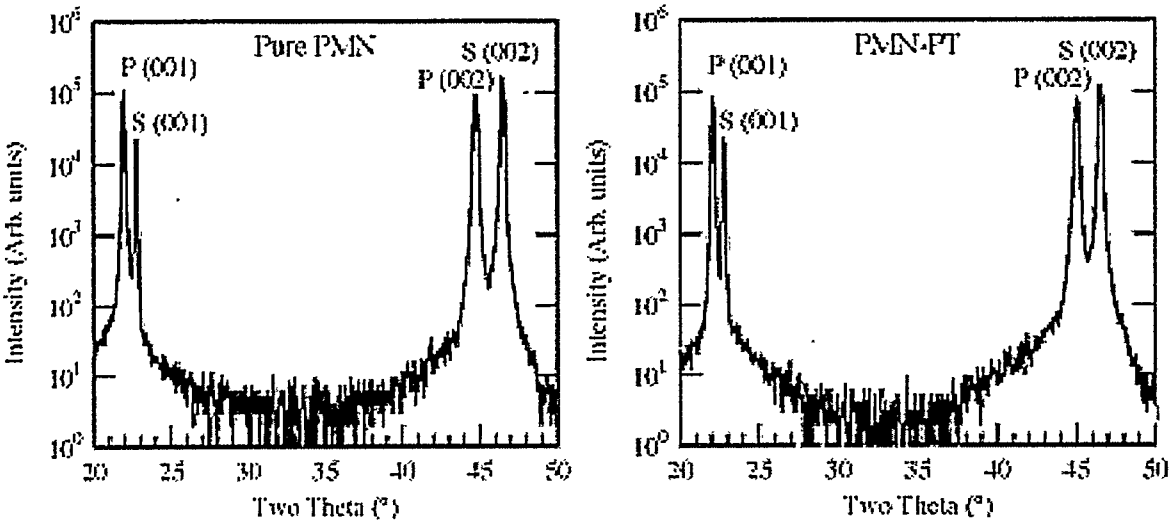


Figure 1. XRD spectrum of a) PMN/$SrTiO_3$ (x=0) and b) PMN-PT/$SrTiO_3$ (x≈0.25) samples grown at 700°C, showing pure (001) orientation. "P" indicates PMN and PMN-PT peaks, respectively. Substrate peaks are indicated by "S".

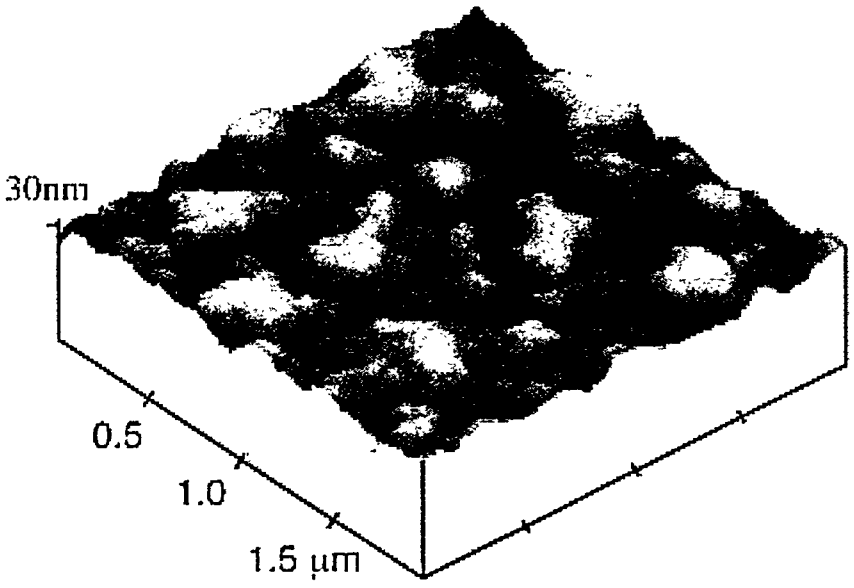


Figure 2. Scanning probe microscope image of the surface of a PMN film deposited on $SrTiO_3$. RMS roughness is 2-3nm.

Typical values for RMS surface roughness of 2-3 nm (over a 2$\mu$m x 2$\mu$m scanned region) were obtained from SPM images of films grown on $SrTiO_3$, Figure 2. A granular surface structure was observed, consistent with the columnar-like microstructure observed in cross-sectional TEM images. Despite the very strong biaxial orientation relationship with the substrate, the films appear to consist of separately nucleated columns distinguished by small in-plane rotations.

The zero-bias permittivity and loss measured at room temperature and 10 kHz for a 220 nm thick pure PMN film deposited at 780°C were 900 and 1.5%, respectively. For PMN-PT films the small-signal permittivity ranged from 1000 to 1500 depending on deposition conditions and Ti content; correspondingly low values for the zero-bias dielectric loss between 1 and 5% were determined for all specimens. Zero-bias permittivities were found to be approximately equal for films grown at both 700°C and 780°C, although asymmetry in the permittivity-field response was frequently observed for films grown at the lower temperature.

Polarization hysteresis loops for samples grown at 780°C are shown in Figure 3. Surprisingly, substantial polarization hysteresis could be observed even for pure PMN films, with a large coercive field. This may result from the very high electric fields that may be applied to these thin films without breakdown, or to the tetragonality imposed by the substrate as discussed above. For films believed to have Ti contents beyond the morphotropic phase boundary, a large reduction in coercive field is observed, Figure 3(c).

We have also obtained the effective $d_{33}$ piezoelectric hysteresis loop using double beam laser interferometry, for a sample grown at 780°C with a PT content of 25-30%. The measurement frequency was 1kHz, and a 0.2Vrms oscillation voltage was used to modulate the sample. A maximum $d_{33}$ of 130-150 pm/V was observed. This compares favorably to high-field $d_{33}$ values obtained on other epitaxial ferroelectric films in this thickness range, but is an order of magnitude smaller than has been obtained in bulk relaxor-based single crystals. Because of the magnitude of the voltage that must be applied to the sample to achieve sufficient signal to noise ratios, the low-field piezoresponse of the PMN-PT film was not probed here. Thus the possible existence of a larger piezoresponse at low field, similar to that observed in single crystals, has not been excluded by these measurements.

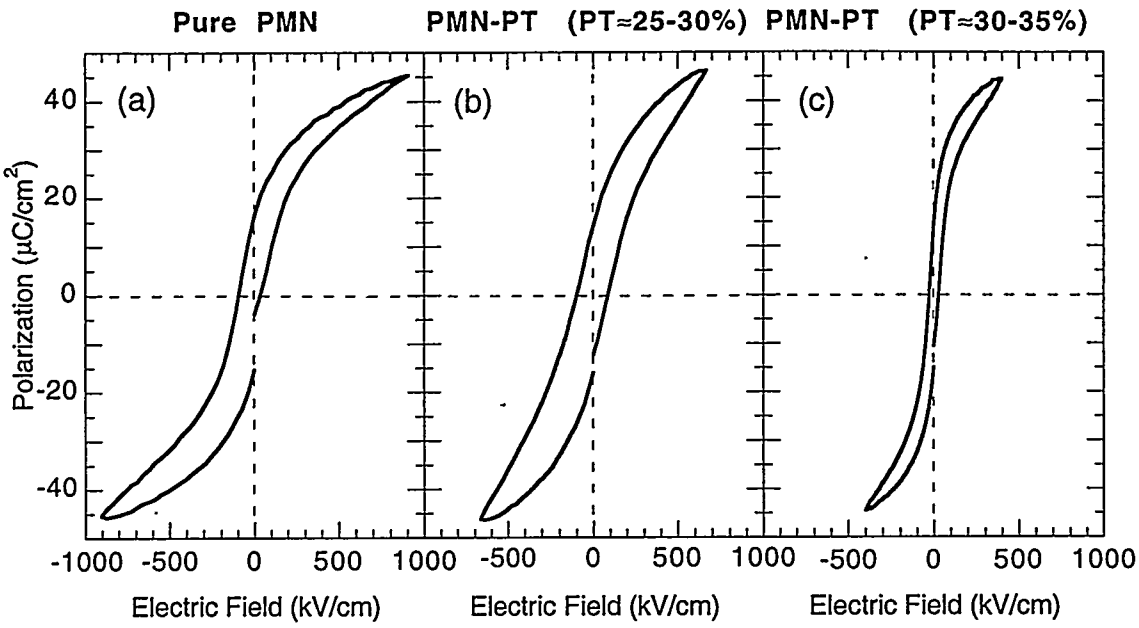


Figure 3. Polarization hysteresis loops for films grown at 780°C for a) 220nm pure PMN; b) 300 nm PMN-PT, x≈0.25-0.3; and c) 250nm PMN-PT, x≈0.3-0.35. Remnant polarization values are a) 16μC/cm², b) 15μC/cm², and c) 18μC/cm².

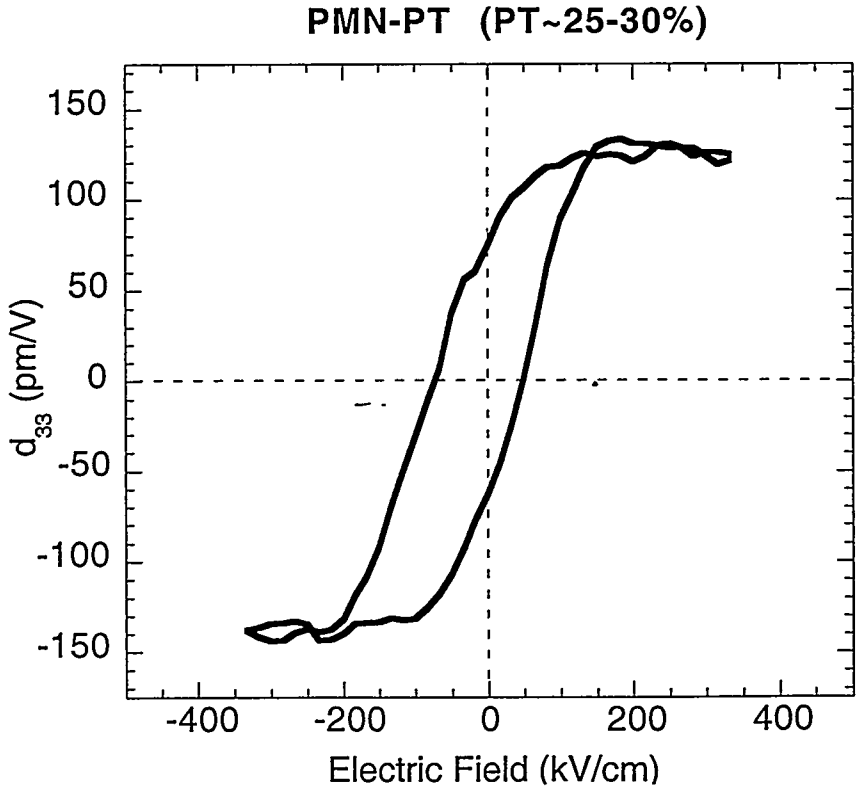

Figure 4. Effective d33 hysteresis loop measured by double-beam interferometry for a 300 nm PMN-PT, x≈0.25-0.3 sample.

## CONCLUSIONS

Nearly phase-pure, epitaxial PMN and PMN-PT films were obtained by MOCVD under proper deposition conditions. The zero-bias dielectric constant and loss measured at room temperature and 10 kHz for 300 nm thick pure PMN films were 900-1400 and 0.01-0.03, respectively. For PMN-PT films the small-signal permittivity ranged from 900 to 1500 depending on deposition conditions and Ti content; low values for the dielectric loss (<0.06) were determined for all specimens. Substantial polarization hysteresis was observed at room temperature both near the morphotropic phase boundary ($P_r$~18μC/cm$^2$) and for pure PMN ($P_r$~16μC/cm$^2$), provided the amplitude of the driving electric field is high enough. Possible explanations for this behavior include the tetragonal biaxial strain imposed on the films by the substrate constraint, and the field-induced development of a stable ferroelectric phase under sufficiently high drive levels.

## ACKNOWLEDGMENTS

This work was supported by the U.S. Department of Energy, BES-Material Sciences, under Contract W-31-109-ENG-38, and by DOE Office of Transportation Technology. We thank Prof. C.-B. Eom of Duke University for providing $SrRuO_3/SrTiO_3$ substrates, and acknowledge many useful discussions with Prof. S. Trolier-McKinstry of Penn State University.

## REFERENCES

1. S. Hirano, T. Yogo, K. Kikuta, K. Kato, W. Sakamoto, and S. Ogasahara, Ferroelectric Films, Ceramic Transactions **25**, edited by A.S. Bhalla and K.M. Nair, American. Cer. Soc., Westerville, 19 (1991).
2. Seung-Eek Park and Thomas R. Shrout, J. Appl. Phys. **82**, 1804-1811 (1997).
3. S. Takashi, A. Ochi, M. Yonezawa, T. Yano, T. Hamatsui, and I. Fukui, Jpn. J. Appl. Phys. **22**, 157 (1993).
4. L.J. Lin and T.B. Wu, J. Am. Ceram. Soc. **74**, 1360 (1991).
5. L.F. Francis and D.A. Payne, J. Am. Ceram. Soc. **74**, 3000 (1990).
6. K.L Saenger, R.A. Roy, D.B. Beach, and K.F. Etzold, MRS Symp. Proc. **285**, 421-426 (1993).
7. Dan Lavric, Rajesh A. Rao, Qing Gan, J.J. Krajewski, and Chang-Beom Eom, Integrated Ferroelectrics **21**, 499-509 (1998).
8. J.-P. Maria, W. Hackenberger, and S. Trolier-McKinstry, J. Appl. Phys. **84**, 5147 (1998).
9. K. R. Udayakumar, J. Chen, P.J. Schuele, L.E. Cross, V. Kumar, and S.B. Krupanishi, Appl. Phys. Lett. **60**, 1187-1189 (1992).
10. L.E. Francis, and D.A. Payne, MRS Symp. Proc. **200**, 173-178 (1990).
11. V.E. Wood, J.R. Busch, S.D. Ramamurthi, and S.L. Schwartz, J. Appl. Phys. **71**, 4557 (1992).
12. M.C. Jiang, T.J. Hong, and T.B. Wu, Jpn. J. Appl. Phys. **33**, 6301 (1994).
13. Y. Takeshima, K. Shiratsuyu, H. Takagi, and K. Tomono, Jpn. J. Appl. Phys. **34** Pt 1, 5083 (1995).
14. C.B. Eom, et al., Science **258**, 1766(1992).
15. G.R. Bai, et al., to be published.
16. C.M. Foster, et al., J. Appl, Phys. **81**, 2349 (1997).

17. S. Stemmer, G.-R. Bai, N.D. Browning, and S.K. Streiffer, submitted to J. Appl. Phys.
18. H. Maiwa, J. A. Christman, S-H. Kim, D-J. Kim, J-P. Maria, B. Chen, S. K. Streiffer, and A. I. Kingon, Jpn. J. Appl. Phys. **38** Pt 1, 5402 (1999).